Gas adsorption in single-walled carbon nanotubes studied by NMR

A. Kleinhammes, S.-H. Mao, X.-J. Yang, X.-P. Tang, H. Shimoda, J. P. Lu, O. Zhou, and Y. Wu*
Department of Physics and Astronomy and Curriculum in Applied and Material Sciences, University of North Carolina, Chapel Hill, North Carolina 27599-3255, USA
(Received 6 February 2003; published 25 August 2003)

Adsorption isotherms of methane and ethane in single-walled carbon nanotubes (SWNTs) were measured by ^{1}H nuclear magnetic resonance (NMR) at room temperature. It is shown that the interior of SWNTs becomes available for methane and ethane adsorption after cutting of SWNTs. Such endohedral adsorption dominates methane and ethane adsorption in SWNTs, at least below 1 MPa. The average exchange time between molecules adsorbed inside SWNTs and free gas molecules outside was estimated to be on the order of 80 ms. It is shown that exposure to oxygen has no effect on methane and ethane endohedral adsorption in SWNTs, suggesting that the adsorption energy of oxygen molecules inside SWNTs is small compared to that of methane. ^{13}C NMR indicates that under atmospheric pressure and room temperature helium atoms could access the interstitial sites of SWNT bundles whereas H_2, CO_2, and N_2 molecules could not.

DOI: 10.1103/PhysRevB.68.075418 PACS number(s): 61.46.+w, 68.43.−h, 82.56.−b

I. INTRODUCTION

Single-walled carbon nanotubes (SWNTs) possess unique nanopore structures making interactions between guest molecules and SWNTs fascinating and important. Such interactions could play an important role in the applications of SWNTs in various areas including gas storage,[1,2] electronic and thermal properties,[3–5] field emission,[6] and biotechnology.[7] A SWNT is formed by rolling a graphene sheet into a seamless cylinder with a diameter on the nanometer scale. These individual SWNTs with similar diameters assemble into bundles in the form of a two-dimensional triangular lattice. Guest molecules could potentially interact with SWNTs via the outer surfaces of bundles, the interstitial channels between the tubes in a bundle, and the inside of the tubes.[8] An important aspect of guest molecule/SWNT interaction is gas adsorption. This is not only important for gas storage but crucial for understanding many other issues such as changes of electronic and thermal properties of SWNTs upon exposure to gases.[3–5] It also provides important information on the nanopore structures of SWNT bundles. For instance, the accessibility of the inside of the tubes for gas adsorption (endohedral adsorption) would depend on the openness of tube ends. Adsorption studies were typically carried out with macroscopic techniques such as volumetric and gravimetric measurements. However, important complementary information, such as molecular dynamics and adsorption sites, could be obtained by microscopic measurements of gas adsorption. Here we describe a study of gas adsorption in SWNTs using NMR. The focus is on the adsorption of methane and ethane in cut SWNTs. It is shown that adsorption inside SWNTs dominates the observed adsorption and the presence of oxygen has no effect on the adsorption of these gases in SWNTs.

II. EXPERIMENT

SWNTs were synthesized by laser ablation and the raw materials were subsequently purified as described in detail elsewhere.[9] Some of the purified SWNTs synthesized using 0.6-at. % (each) Ni/Co as catalysts were cut to shorter tubes by sonication in a 3:1 ratio of H_2SO_4 and HNO_3 solutions for 24 h.[10] The average length of cut SWNTs is about 0.5 μm. Both the cut and uncut SWNTs are in the form of bundles with average diameters of about 12 nm obtained by examining pictures of transmission electron microscopy. These samples are over 90% pure SWNTs. A SWNT sample made with 2.4-at. % (each) Rh/Pd as catalysts was also used in this study. The average diameter of the nanotubes estimated by Raman measurements is 1.4 nm in samples made with 0.6-at. % (each) Ni/Co as catalysts and 0.85 nm in the sample made with 2.4-at. % (each) Rh/Pd as catalysts.[9] The section of the quartz NMR sample tube within the NMR coil has a volume of 5.3×10^{-2} cm^3 and is filled up with 15 mg of SWNTs. For a SWNT diameter of 1.4 nm and an average bundle size of 12 nm (about 37 SWNTs per bundle), the estimated specific density of such a close-packed SWNT bundle is 1.33 g/cm^3. Therefore, SWNTs of 15 mg would occupy an estimated volume of only 1.2×10^{-2} cm^3, with 20% of the 5.3×10^{-2}-cm^3 NMR sample tube volume within the NMR coil. Thus, although the SWNTs spread out over the entire volume of the sample space, the sample packing was not dense. For gas loading, the NMR sample tube was connected to a stainless-steel tubing vacuum system connected to various pressurized gas sources. The system was leak-tested rigorously. No increase of NMR proton signal was detected after several days with the sample under vacuum but without dynamic pumping. All ^{1}H NMR measurements were carried out at room temperature (RT) in either a superconducting magnet of 4.7 T or an iron magnet of 0.8 T. All samples were first annealed at 400 °C for 1 h at 5×10^{-6} torr in the quartz NMR sample tube before NMR measurements.

III. RESULTS AND DISCUSSION

A. Adsorption isotherms

Figure 1 shows RT ^{1}H spectra of cut SWNTs exposed to methane and ethane, respectively, at a pressure of 0.045 MPa. Both spectra have a sharp peak and a broad peak. The

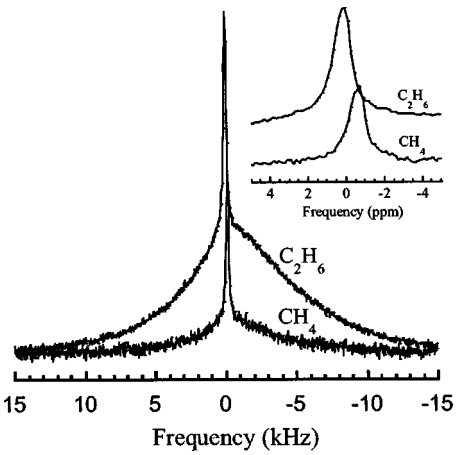

FIG. 1. RT ^{1}H spectra of cut SWNTs exposed to 0.045-MPa CH_4 and C_2H_6 measured at 4.7 T. The central narrow peaks (see inset) represent gas molecules in the free space between SWNT bundles in the NMR tube. The observed chemical shift difference of 0.75 ppm is characteristic of the two gases. The broad peaks represent gas molecules adsorbed on SWNTs. Both the broad and narrow peaks can be fit with Lorentzian lines.

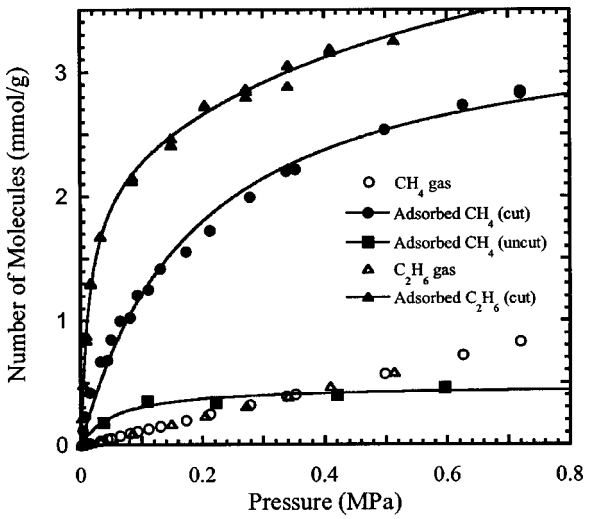

FIG. 2. Pressure dependence of the intensities of the narrow (free gas) and broad (adsorbed) peaks of the ^{1}H spectra (see Fig. 1) of cut SWNTs exposed to CH_4 and C_2H_6 at RT. For comparison, CH_4 adsorption in uncut SWNTs at RT is also shown. Both the cut and uncut SWNT samples were produced under the same conditions. The solid lines are Langmuir-type adsorption curve fits discussed in the text. No significant hysteresis effect was observed for the adsorption curves. The unit of adsorption is mmol per gram, that is, the number of mmol adsorbent molecules per gram of SWNTs. A multiplication factor of 1.33 g/cm^3, the density of the maximum-packed SWNT sample, converts the unit to mmol/cm^3. For the gas peak, the intensity is the number of mmol of free gas molecules in our NMR sample tube divided by 0.015 g of SWNTs. A factor of 15×10^{-3} g/4.1×10^{-2} cm^3 converts the gas peak intensity to a gas density in units of mmol/cm^3.

sharp peak is attributed to gas molecules in the region of the NMR sample tube unoccupied by SWNTs, with about 80% of the sample tube volume within the NMR coil. Figure 2 shows the intensities of these two peaks versus pressure for both methane and ethane. The intensity of the sharp peak is proportional to the pressure, consistent with ideal gas behavior. The chemical shift difference of 0.75 ppm between the sharp peaks in the ethane and methane proton spectra, as shown in the inset of Fig. 1, is in perfect agreement with the expected chemical shift difference between free ethane and methane gas molecules. To further confirm the negligible contribution of adsorption to this sharp peak we compared this sharp peak intensity for CH_4, C_2H_6, and H_2. In all three cases, the measured intensity of the sharp peak corresponds to the same number of molecules at the same pressure. Since the adsorption energy of H_2 on SWNTs is expected to be much smaller than that of C_2H_6 and CH_4,[11,12] this proves that the contribution of adsorbed molecules to this sharp peak is negligible. The absolute number of molecules associated with this sharp peak can be calculated by assuming an ideal gas occupying a volume of 4.1×10^{-2} cm^3 (80% of the NMR sample space volume).

In contrast to the sharp peak, the broad peak in Fig. 1 shows characteristic behaviors of adsorption. Its intensity increases nonlinearly with pressure as shown in Fig. 2. An analytical description of such an adsorption isotherm, although an oversimplified one, is Langmuir adsorption described by[13]

$$n(P,T)=n_\infty\frac{bP}{1+bP}, \tag{1}$$

where $n(P,T)$ is the number of adsorbed molecules as a function of pressure P and temperature T, n_∞ is the number of adsorption sites, and b is given by[13]

$$b=\frac{\sigma}{\nu_0\sqrt{2\pi m k_B T}}\exp(E_d/k_BT), \tag{2}$$

where σ is the effective area covered by an adsorbed molecule with mass m, and k_B is the Boltzmann constant. ν_0 is the prefactor of the desorption rate constant $k=\nu_0\times\exp(-E_d/k_BT)$ with a typical value of $\nu_0=1\times10^{13}$ s^{-1}, and E_d is the activation energy of desorption. The adsorption isotherm of methane can be fit by Eq. (1) with $E_d=235\pm2$ meV (22.7 kJ/mol) and $n_\infty=3.5\mp0.2$ mmol/g as shown in Fig. 2. For this fitting $\sigma=1.6\times10^{-19}$ m^2 was used based on the bulk liquid density of methane. Measurement of endohedral adsorption of supercritical methane in SWNTs has not been reported previously. Calculations based on nonlocal density-functional theory (DFT) and grand canonical Monte Carlo (GCMC) simulation showed that endohedral adsorption of supercritical methane in a SWNT of diameter 1.4 nm deviates strongly from linear pressure dependence at 1 MPa where the level of saturation is nearly achieved.[14,15] In contrast to the calculated endohedral adsorption, the calculated adsorption on the outside of the SWNT shows linear pressure dependence up to 1 MPa with no effect of saturation.[14] Thus, the strongly nonlinear pressure dependence of the broad peak intensity is inconsistent with adsorption on the outside of bundles and is consistent with endohedral adsorption based on DFT and GCMC simulations. The observed number of

adsorbed CH_4 molecules shown in Fig. 2 is also consistent with what was expected from filling the inside of SWNTs as evidenced by the good agreement with GCMC simulations for endohedral adsorption of (10,10) SWNTs (Ref. 15) and SWNTs with a diameter of 1.4 nm.[14] It is interesting to note that the activation energy $E_d = 235$ meV is comparable to the observed adsorption energy of 222 meV associated with the groove sites of SWNT bundles.[16,17] The concave curvature of endohedral adsorption sites could lead to increased adsorption energy as compared to that on graphite. Similarly, the effective concave curvature of the grooves on SWNT bundles could also lead to such enhancement. The adsorption energy of groove sites is the largest among all other adsorption sites on the external surface of SWNT bundles. However, the number of groove sites is much smaller than that of endohedral adsorption sites in our sample. The derived activation energy E_d should only be considered as a crude estimate of the adsorption energy of endohedral sites because of the oversimplified nature of the Langmuir adsorption isotherm. There are other uncertainties such as the prefactor ν_0 which could deviate somewhat from 1×10^{13} s^{-1} as assumed in the fitting.[18]

Since an ethane molecule contains more atoms than methane, the adsorption energy of ethane is expected to be larger than that of methane on the same surface. The reported adsorption energy of methane on a graphite surface is 126 meV whereas that of ethane is 170–190 meV.[19] The adsorption isotherm of the broad peak for ethane shows that this is indeed the case. Figure 2 shows that significant adsorption of ethane occurs at much lower pressure compared to methane. The fitting of the adsorption isotherm, however, requires two components with different activation energies. The component with higher activation energy is well constrained by the data with $E_d = 303 \pm 15$ meV (29.2 kJ/mol) and $n_\infty = 2.2 \mp 0.2$ mmol/g. Here, $\sigma = 2.0\times10^{-19}$ m^2 was used in the fitting based on the bulk liquid density of ethane. Because of the lack of data at higher pressure, the component with lower adsorption energy around 200 meV is not well constrained and has a very large degree of freedom in the fitting parameters of E_d and n_∞. Obviously, the fitting procedure here does not necessarily imply the existence of two adsorption sites for ethane. The functional form of the adsorption isotherm for the current case needs to be calculated using DFT and GCMC simulations. Langmuir adsorption is an oversimplified description for endohedral adsorption in SWNTs where molecular interactions are expected to be dependent on the degree of loading inside the tubes. Nevertheless, the Langmuir fitting analysis provides some useful information for comparing the adsorption data of methane and ethane. The adsorption of methane in the pressure range of current experiments corresponds to the portion of ethane adsorption described by the component with $E_d = 303$ meV. The ratio of 303 meV and 235 meV is comparable to the ratio of the adsorption energies of ethane and methane on a graphite surface. The component with smaller adsorption energy for ethane does not have a corresponding component in the observed methane adsorption isotherm. This is fully expected since the corresponding component for methane would have much lower adsorption energy and will not contribute significantly to the adsorption isotherm in the pressure range of current experiments. It is worth pointing out that adsorption on residual Ni/Co particles cannot contribute to the observed adsorption by NMR since the magnetic effect on such magnetic particle surfaces will wipe out the NMR signals. Also, under the current experimental conditions, no evidence of molecular hydrogen adsorption was observed by NMR.

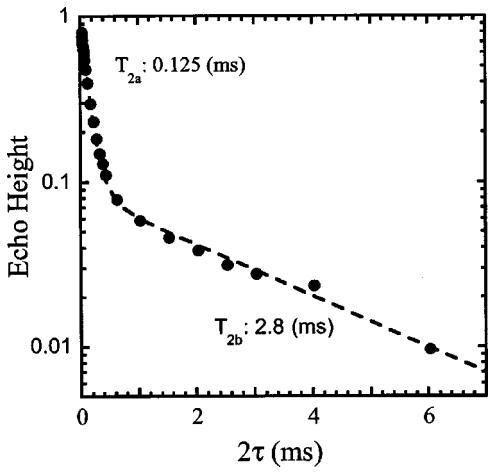

FIG. 3. Decay of the ^1H Hahn-echo intensity at RT as a function of dephasing time 2τ measured for C_2H_6 gas at 0.093 MPa in contact with cut SWNTs (4.7 T). Clearly, there are two components in the echo decay. The dashed line is a fit using double exponential decays. The component with $T_{2a} = 0.125$ ms is associated with molecules adsorbed inside SWNTs whereas the much longer $T_{2b} = 2.8$ ms corresponds to free gas molecules.

B. Spin-spin and spin-lattice relaxations

The spin-spin relaxation was measured with the Hahn-echo pulse sequence 90°-τ-180°-τ-echo.[20] Figure 3 shows the decay of the Hahn-echo height S_{echo} as a function of the dephasing time 2τ for ethane at 0.093 MPa measured at 4.7 T. It clearly shows two components of exponential decays described by $S_{echo} = a\exp(-2\tau/T_{2a}) + b\exp(-2\tau/T_{2b})$ where a and b are the intensities and T_{2a} and T_{2b} are the spin-spin relaxation times of the two components. The fitting shows that $T_{2a} = 125 \pm 3$ μs and $T_{2b} = 2.8 \pm 0.1$ ms. Analysis of the spectrum corresponding to each 2τ value shows that the $T_{2a} = 125$ μs component corresponds to the broad peak and the $T_{2b} = 2.8$ ms component corresponds to the sharp peak. The ratio a/b is exactly the same as the intensity ratio of the broad and sharp peaks of the spectrum. Within experimental error, T_{2a} does not depend on the pressure or the magnetic field. For methane the observed $T_{2a} = 160 \pm 10$ μs is also independent of the pressure and the magnetic field. T_2 in porous media could originate from diffusion-induced local-field variation due to a magnetic-susceptibility effect.[21] In general, such fluctuations can be reduced by carrying out measurements at low magnetic field where the magnetic-susceptibility effect is reduced. The reason that such field dependence did not occur for T_{2a} can be understood by analyzing the origin of the line broadening for the broad peak. A small amount of Co/Ni magnetic particles exist in SWNT

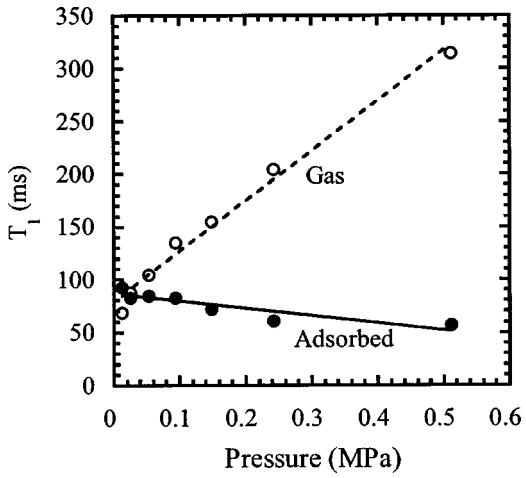

FIG. 4. Pressure dependence of the spin-lattice relaxation time T_1 for C_2H_6 gas in contact with cut SWNTs (4.7 T). The T_1 of the free gas in the NMR tube (narrow peak) shows a linear increase with pressure characteristic of gas systems. The broad peak representing the adsorbed molecules displays a slight decrease with pressure in T_1. Note that the relaxation times for the two species that are diverging with increasing pressure coincide at low pressure hinting at a possible exchange between gas and adsorbed molecules at low pressure on a T_1 time scale.

samples even after purification and cutting. Such magnetic particles produce a distribution of local fields throughout the sample. For gas molecules moving rapidly throughout the sample space, such local-field distribution is averaged out over the NMR time scale leading to the sharp resonance peak. For adsorbed molecules confined in space over the NMR time scale, molecules experience different local fields depending on their locations. This local-field distribution causes line broadening. As long as the external magnetic field is larger than the coercive field of the magnetic particles, the local-field distribution caused by such magnetic particles is independent of the external magnetic field. The line shape of the broad peak can be fit very well by a Lorentzian line. The full-width-at-half-height (FWHH) linewidths are 7.5 ± 0.5 kHz and 7.0 ± 0.5 kHz for the spectra taken at 4.7 and 0.8 T, respectively. The effect of $T_2=125$ μs contributes to a Lorentzian line broadening of FWHH $=2.5$ kHz. Clearly, the local field is dominated by the contribution of magnetic particles. This explains the observed independence of the broad peak T_2 on the external magnetic field. The small difference of the broad peak T_2 for methane and ethane is most likely due to the different diffusion rate of methane and ethane inside SWNTs.[22]

Spin-lattice relaxation was also measured for both the sharp and broad peaks. Spin-lattice relaxation time T_1 was determined by measuring the recovery rate of the nuclear magnetization (M) after saturation. Here, M was measured as a function of recovery time t after saturation and T_1 is the time constant of the curve $M^*(t)=1-M(t)/M(\infty)$. Figure 4 shows the T_1 values of both the sharp and broad peaks of ethane as a function of pressure measured at 4.7 T. As expected from the well-known NMR properties of gases in the fast motion limit,[23] T_1 of the gas phase peak increases linearly with pressure due to the increased rate of molecular collision. However, the straight line of T_1 versus P does not go through the origin (0,0) when extrapolated to zero pressure. This is most likely due to molecular collisions with walls of SWNT bundles in the porous sample space. Here, T_1 is determined by $T_1=\alpha_{gas}P+R_{wall}$ where the first term is proportional to the pressure-dependent collision rate of a gas molecule with other gas molecules and the second term is proportional to the collision rate of a gas molecule with walls of SWNT bundles. The last term is independent of pressure. Unlike the sharp peak, T_1 of the broad peak decreases slightly with increasing pressure. The much weaker pressure dependence of T_1 is consistent with adsorption although the relaxation mechanism remains to be determined. It is interesting, however, that the T_1 values of the broad and sharp peaks merge toward a common value at low pressure. This seems to indicate that molecules in the gas phase and the adsorbed phase undergo sufficient exchanges at low pressure on the T_1 time scale of about 80 ms. Two-dimensional exchange spectroscopy needs to be carried out for further investigation.

C. Endohedral adsorption

As discussed earlier, the adsorption isotherms are consistent with endohedral adsorption. The properties of the spin systems also support this assignment. When the adsorbed phase and the gas phase are in equilibrium, adsorbed molecules and gas molecules undergo rapid exchanges due to adsorption and desorption. The residence time t_s of a molecule adsorbed on the surface before desorbing into the gas phase can be estimated by[13]

$$t_s=10^{-13}\ \mathrm{s}\exp(E_d/k_BT). \tag{3}$$

For $E_d=235$ meV and $T=300$ K, $t_s=9\times10^{-10}$ s. The average time t_g a molecule spends in the gas phase can be estimated by $N_g/t_g=N_s/t_s$ where N_g and N_s are the number of gas and adsorbed molecules involved in the exchange, respectively. The exchange rate between the gas and adsorbed molecules is given by $R_{exch}=1/(t_g+t_s)$. If the broad peak (Fig. 1) was due to adsorption on a surface which is in direct contact with the gas phase, such as the surface of SWNT bundles, N_g and N_s would be on the same order of magnitude (Fig. 1) and t_g would be comparable to t_s. Therefore, $1/R_{exch}$ would be much shorter than the free-induction decay time scale of 100 μs and only one resonance peak would be observed by NMR due to rapid exchange. This is clearly not the case as shown in Fig. 1. It is worth mentioning that despite the uncertainty with regard to the value of E_d, the residence time is undoubtedly much shorter than the NMR time scale. For instance, even with $E_d=400$ meV, the estimated residence time of $t_s=5\times10^{-7}$ s would still be much shorter than the free-induction decay time scale. The two distinguished T_2 values for the adsorbed and gas peaks indicate also that the time scale of exchange is longer than 100 μs. In fact, the two distinguished T_1 values at higher loading (Fig. 4) indicate that the exchange time could be comparable to 80 ms. This is inconsistent with adsorption on a surface which is in direct contact with the gas phase. The

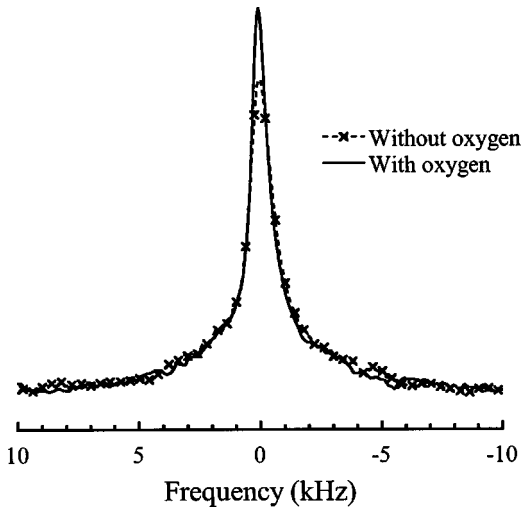

FIG. 5. ^{1}H spectrum of cut SWNTs exposed to 0.055-MPa CH_4 measured at 0.8 T and RT. Also shown is a ^{1}H spectrum measured at 0.8 T and RT obtained by first exposing cut SWNTs to 0.079-MPa O_2 and then adding CH_4 which has a partial pressure of 0.055 MPa. The two spectra are virtually identical. The small difference in the gas peak height is due to a slightly larger line broadening of the spectrum with oxygen due to magnetic-field drift of the iron magnet. This drift is also responsible for the broader appearance of the gas peaks compared to that in Fig. 1.

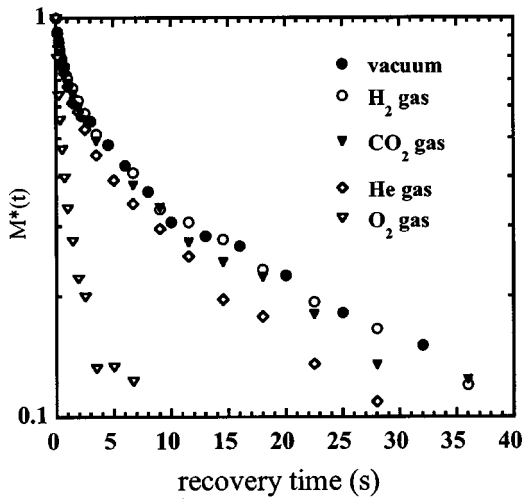

FIG. 6. ^{13}C saturation recovery curve measured for SWNTs (10% enriched in ^{13}C, uncut, Pd/Rh catalysts) at 9.4 T. ^{13}C nuclei on SWNTs in vacuum, exposed to H_2, CO_2, and N_2 (not shown for clarity) gases at 0.17 MPa show the same relaxation behavior. Exposure to 0.17-MPa O_2 increases the relaxation rate dramatically while exposure to He gas induces a modest but significant rate increase. Paramagnetic O_2 might cause increased relaxation due to the interaction of its electron spin with ^{13}C nuclear spins. Helium gas will only affect the relaxation of all ^{13}C spins if He atoms are able to penetrate into the bundle network either through the interstitial channels or through defects on the walls of SWNTs.

long exchange time is consistent with endohedral adsorption. There, adsorbed molecules could not be desorbed directly into the gas phase without exiting the ends of SWNTs. Thus, the effective number of N_s involved in the exchange is extremely small (on the order of the number of tube ends). This makes t_g extremely long according to $t_g = t_s N_g / N_s$. This supports again the assignment of the observed adsorption to endohedral adsorption. Further support for the assignment of endohedral adsorption comes from the NMR adsorption measurement of methane in an uncut SWNT sample produced under the same conditions as the cut SWNT sample. The result is shown in Fig. 2. Here, the adsorption isotherm has a very similar functional form and apparent adsorption energy as that in the cut SWNT sample. However, the level of adsorption is about ten times smaller. This is consistent with the understanding that the ends of most SWNTs are capped without cutting. A small fraction of SWNTs are accessible for endohedral adsorption due to defective walls or ends.

D. Effects of exposure to oxygen and other gases

In order to evaluate the influence of oxygen on adsorption of methane and ethane in SWNTs, competitive adsorption between O_2 and methane and between O_2 and ethane were studied. Figure 5 shows a proton spectrum under exposure of 0.055-MPa pure methane. Also shown is a proton spectrum obtained by first exposing SWNTs to 0.079-MPa O_2 and then adding methane with a partial pressure of 0.055 MPa. The two spectra are virtually identical. Similar experiments were done also with ethane and no effect of O_2 on ethane adsorption was observed. This experiment demonstrates that endohedral adsorptions of methane and ethane are stronger than endohedral adsorption of O_2 in SWNTs. This is consistent with recent measurements and calculations showing that adsorption energy of O_2 in SWNTs is small.[24,25]

There is an additional feature associated with gas adsorption in SWNTs. That is, if gas molecules could access the interstitial sites of the bundles, all carbon atoms could be accessed by gas molecules. As a result, ^{13}C NMR could be affected upon exposure to gas molecules. Figure 6 shows the changes of the ^{13}C saturation recovery curve upon exposure to different gases in an uncut SWNT sample made with 2.4-at. % (each) Rh/Pd as catalysts. It is clear that oxygen has a dramatic effect on the relaxation behavior. We believe that this effect is due to the fact that oxygen molecules are paramagnetic. Magnetic-field fluctuations caused by O_2 create an additional channel for energy relaxation of ^{13}C nuclear spins. Since ^{13}C relaxation time is very long, the effect of O_2 is quite significant. In contrast, exposures of SWNTs to 0.17-MPa CO_2, H_2, and N_2 have no effect on ^{13}C spin-lattice relaxation. It is interesting to note that exposure to 0.1-MPa helium does have a noticeable effect on ^{13}C spin-lattice relaxation. This means that He could access the majority of carbon atoms in uncut SWNTs. The perturbation of the electron cloud around carbon due to collisions with He atoms could contribute to spin-lattice relaxation. This shows that He atoms can access the interstitial sites of the bundles whereas CO_2, H_2, and N_2 cannot. The effect of helium is consistent with previous studies.[5,26,27]

IV. CONCLUSIONS

The reported study shows that NMR is an effective tool for studying gas adsorption in SWNTs. Proton NMR shows

that the interior of SWNTs becomes available for methane and ethane adsorption after cutting of SWNTs. Such endohedral adsorption dominates methane and ethane adsorption in SWNTs below 1 MPa. The observation agrees with calculations of endohedral adsorption using DFT and GCMC simulations. It was found that exposure to oxygen has no effect on methane and ethane endohedral adsorption in SWNTs. This suggests that the adsorption energy of oxygen molecules inside SWNTs is smaller than that of methane. No evidence of adsorbed molecular hydrogen was found by NMR under the current experimental conditions. ^{13}C NMR indicates that helium could access the interstitial sites of SWNT bundles whereas H_2, CO_2, and N_2 molecules cannot under atmospheric pressure.

ACKNOWLEDGMENTS

This work was supported by ONR MURI Contract No. N00014-98-1-0597, the NSF Contract No. DMR-0139452, and ACS-PRF Contract No. 37310-ACS.

*Author to whom correspondence should be addressed. Email address: yuewu@physics.unc.edu

[1] M. Schlapbach and M. Züttel, Nature (London) **414**, 353 (2001).
[2] M. Hirscher, M. Becher, M. Haluska, A. Quintel, V. Skakalova, Y. M. Choi, U. Dettlaff-Weglikowska, S. Roth, I. Stepanek, P. Bernier, A. Leonhardt, and J. Fink, J. Alloys Compd. **330**, 654 (2002).
[3] J. Kong, N. R. Franklin, C. W. Zhou, M. G. Chapline, S. Peng, K. J. Cho, and H. J. Dai, Science **287**, 622 (2000).
[4] P. G. Collins, K. Bradley, M. Ishigami, and A. Zettl, Science **287**, 1801 (2000).
[5] G. U. Sumanasekera, C. K. W. Adu, S. Fang, and P. C. Eklund, Phys. Rev. Lett. **85**, 1096 (2000).
[6] Y. Saito, T. Nishiyama, T. Kato, S. Kondo, T. Tanaka, J. Yotani, and S. Uemura, Mol. Cryst. Liq. Cryst. **387**, 303 (2002).
[7] M. Shim, N. W. S. Kam, R. J. Chen, Y. M. Li, and H. J. Dai, Nano Letters **2**, 285 (2002).
[8] M. M. Calbi, M. W. Cole, S. M. Gatica, M. J. Bojan, and G. Stan, Rev. Mod. Phys. **73**, 857 (2001).
[9] X.-P. Tang, A. Kleinhammes, H. Shimoda, L. Fleming, K. Y. Bennoune, S. Sinha, C. Bower, O. Zhou, and Y. Wu, Science **288**, 492 (2000).
[10] H. Shimoda, B. Gao, X.-P. Tang, A. Kleinhammes, L. Fleming, Y. Wu, and O. Zhou, Phys. Rev. Lett. **88**, 015502 (2002).
[11] G. Stan, M. J. Bojan, S. Curtarolo, S. M. Gatica, and M. W. Cole, Phys. Rev. B **62**, 2173 (2000).
[12] J. Zhao, A. Buldum, J. Han, and J. P. Lu, Nanotechnology **13**, 195 (2002).
[13] J. H. de Boer, *Dynamical Character of Adsorption* (Oxford University Press, London, 1968).
[14] H. Tanaka, M. El-Merraoui, W. A. Steele, and K. Kaneko, Chem. Phys. Lett. **352**, 334 (2002).
[15] A. I. Skoulidas, D. M. Ackerman, J. K. Johnson, and D. S. Scholl, Phys. Rev. Lett. **89**, 185901 (2002).
[16] S. E. Weber, S. Talapatra, C. Journet, A. Zambano, and A. D. Migone, Phys. Rev. B **61**, 13 150 (2000).
[17] S. Talapatra and A. D. Migone, Phys. Rev. B **65**, 045416 (2002).
[18] K. A. Fichthorn and R. A. Miron, Phys. Rev. Lett. **89**, 196103 (2002).
[19] G. Vidali, G. Ihm, H.-Y. Kim, and M. W. Cole, Surf. Sci. Rep. **12**, 133 (1991).
[20] C. P. Slichter, *Principles of Magnetic Resonance* (Springer-Verlag, Berlin, 1989).
[21] P. T. Callaghan, *Principles of Nuclear Magnetic Resonance Microscopy* (Clarendon, Oxford, 1991).
[22] Z. Mao and S. B. Sinnott, J. Phys. Chem. B **104**, 4618 (2000).
[23] A. Abragam, *Principles of Nuclear Magnetism* (Oxford University, New York, 1985).
[24] H. Ulbricht, G. Moos, and T. Hertel, Phys. Rev. B **66**, 075404 (2002).
[25] A. Ricca and J. A. Drocco, Chem. Phys. Lett. **362**, 217 (2002).
[26] W. Teizer, R. B. Hallock, E. Dujardin, and T. W. Ebbesen, Phys. Rev. Lett. **82**, 5305 (1999).
[27] W. Teizer, R. B. Hallock, E. Dujardin, and T. W. Ebbesen, Phys. Rev. Lett. **84**, 1844 (2000).